

Breast Cancer Histopathological Image Classification: Is Magnification Important?

Vibha Gupta, Arnav Bhavsar

vibha.gupta@students.iitmandi.ac.in, arnav@iitmandi.ac.in

School of Computer and Electrical Engineering,
Indian Institute of Technology Mandi, Mandi, India

Abstract

Breast cancer is one of the most common cancer in women worldwide. It is typically diagnosed via histopathological microscopy imaging, for which image analysis can aid physicians for more effective diagnosis. Given a large variability in tissue appearance, to better capture discriminative traits, images can be acquired at different optical magnifications. In this paper, we propose an approach which utilizes joint colour-texture features and a classifier ensemble for classifying breast histopathology images. While we demonstrate the effectiveness of the proposed framework, an important objective of this work is to study the image classification across different optical magnification levels. We provide interesting experimental results and related discussions, demonstrating a visible classification invariance with cross-magnification training-testing. Along with magnification-specific model, we also evaluate the magnification independent model, and compare the two to gain some insights.

1. Introduction

Breast cancer remains one of the major concerns in the medical field and the fifth most common cause of cancer mortality among women worldwide [1]. A biopsy followed by microscopic examination is a vital technique for reliable detection of breast cancer [2]. In a biopsy, a small sample of cells or tissue is removed from the body and then dyed with stain (H & E) that highlights the nuclei by binding DNA (dark purple colour) and other structures by binding proteins (pink colour) [3]. After the staining, glass slides (tissues) are sent to the lab where microscopic examination of tissues is carried out by pathologist. Histopathology imaging has been a ‘gold standard’ in diagnosing almost all types of cancers because it captures a more comprehensive view of the disease [4].

Due to the increase in the number of cancer patients

day by day, the diagnosis can be tedious and also hampered by observer variability. Thus, there is a pressing need of computer-aided diagnosis (CADx) system to relieve the pathologist workload such that attention can be focused on the most suspicious cases, and to overcome the subjective interpretation in order to get the reliability of the obtained results.

The problem of breast cancer histopathology image classification could be addressed in two ways, one is with segmentation and other without segmentation. While some segmentation approaches have been reported, the accurate segmentation is still a challenging problem due to the inherent diversity of the appearance of epithelial cancerous cell or in general, variability of the tissue appearance [3]. Additionally, nuclei may be tightly clumped, overlapped which makes this task even more difficult.

Thus, various methods that do not rely on segmentation have also been proposed. These methods directly extract the features from images and apply the classification framework to classify the issues as malignant/benign [5, 6, 7, 8, 9, 10].

Even for segmentation-free image classification, we assert that there are two factors which may dictate the performance of the system:

- The high degree of variability in tissue appearance mainly due to irregularity in the staining process. Variability in the appearance may exist depending on differences in staining protocol such as differences in fixation, inconsistency in the staining condition and reagents, between labs as well as in the same lab. In other words, we can say that histopathology images exhibit significant inhomogeneity in colour and texture.
- The images can be captured at different optical magnification levels, where each magnification can represent different information. The lowest magnification captures the larger region of interest (ROI), while other magnifications capture the zoomed-in view of tissue inside the initial ROI. Using different magnifications

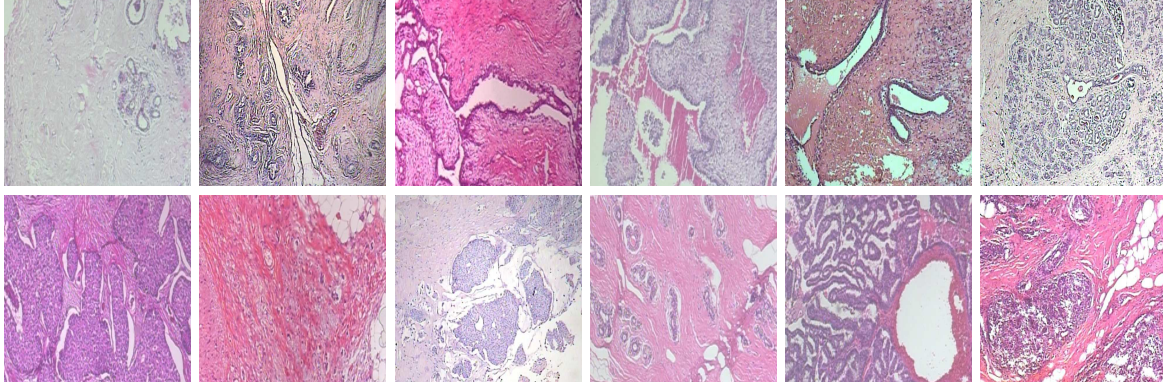


Figure 1. Sample of histopathological images (first row: benign tumor, second row: malignant tumor) from BreakHis dataset at magnification factor of 40X.

can potentially yield varying discriminative information for the classification task. However, some questions are yet unanswered. For instance, is there a magnification model which is more useful for classification, is it useful to define models which consider all magnifications, and if so, how ?

Recently, Spanhol et al. [10] released the BreakHis dataset, thus providing a benchmark data to explore directions to address the above concerns. The BreakHis dataset contains 7909 microscopic biopsy images that were collected from 82 patients in four different magnifications (40x,100x,200x,400x). Figure 1 shows the some sample images of BreakHis dataset caputed at lowest magnificaion (40X). First and second row in figure show the samples of benign and malignant cases respectively. Figure 2 shows the images of different magnification captured from single slide (malignant).

With regards to the first of the above concerns, it is desirable that methods should be able to capture the appearance (colour and texture) variability, which is attempted in the approaches cited above.

Zhang et al. [5] investigated multiple image descriptors along with random subspace ensembles and proposed two-stage cascade framework with a rejection option. In another work [6], an ensembles of one-class classifiers were assessed by the same authors. Bahlmann et al. [7], colour transformed the RGB patch into two channels, called H and E that intensify the hematoxylin (eosin) at the same time suppressing eosin (hematoxylin) stain. They extracted the feature vector of dimension 22 and used liner classifier to diagnose relevant or irrelevant regions. In [8], similar approach was applied for segmentation and classification. Linder et al. [9] extracted the local binary pattern combined with a contrast measure (LBP/C) and evaluated the performance using support vector machine (SVM). However, we note that these methods use independent dataset (not public), and not the BreakHis dataset for validation. However,

in the studies associated with the dataset [10], a series of experiments utilizing six different state-of-art texture descriptors such as Local Binary Pattern (LBP), Completed Local Binary Pattern (CLBP), Threshold Adjancecy Statistics (PFTAS), Grey-Level Co-occurence Matrix (GLM), Local Phase Quantization (LPQ), Oriented FAST and rotated BRIEF (ORB), and four different classifiers were evaluated and showed the accuracy at patient level. In [11], Alexnet [12] was used for extracting features and classification.

We believe that the colour-texture variability can be better captured with integrated colour-texture features [13]. Such features intricately connect texture and colour information by considering the mutual dependency of colour and texture information. These features can be defined with individual colour channels, or with correlated pairs of colour channels. Such, robust integration of colour and texture features can locally adapt to the variation in the image content [14].

With regards to the magnification related concerns, some existing approaches have explored different strategies for classification. In [10, 11], authors reported results on magnification-specific models. However, it would seem that one magnification model may not be able to handle images with other magnifications, and different classifiers are required at different magnifications. Moreover, decision in such cases where large variation in patient score exists, may not be reliable by just considering one magnification level.

To address these concerns, Bayramoglu at el. [15] proposed a magnification independent model utilizing deep learning to classify the benign and malignant cases. The magnification independent system is trained with images of different magnifications, and thus can handle the scale diversity in microscopic images.

Considering these two strategies, in this work, we question about how much does the variation in magnification affect the classification performance of the system, and in this respect, we demonstrate some interesting experimen-

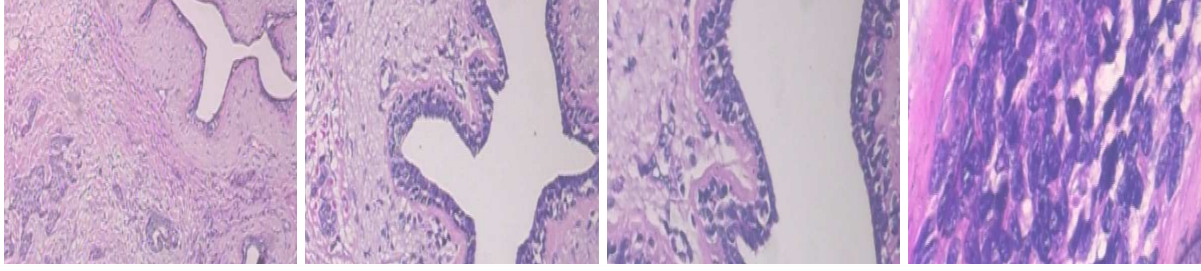


Figure 2. A ductal carcinoma (malignant tumor) acquired at different magnification factors: 40X, 100X, 200X, and 400X.

tal results. From an academic perspective, we believe that such a study opens up further directions of inquiry about features which are largely invariant, or which can be made so, by some classifiers. From a practical standpoint, such a question is important from the point of view of deploying systems in under-developed or developing countries (e.g. in rural areas), which may have limited microscopy facilities.

More specifically, we train a model at specific magnifications and test it with the images of different magnifications. Further, we compare such cross-magnifications studies with the magnification-independent model, which is trained and tested with images of all magnifications. Different from [10, 11] and [15] in this work, we utilize the fusion of colour-texture features, and an ensemble of heterogeneous classifiers followed with majority voting. The reason behind using ensemble is that different classifiers can yield different performance for each magnification.

The rest of the paper is organized as follows: A description of BreakHis dataset is provided in section 2. Section 3 explains the methodology which includes the description of colour-texture features and classifiers, and majority voting. The experiments and results are discussed in section 4.

2. Dataset

The BreakHis dataset [10] consists of 7909 microscopic biopsy images divided into benign and malignant breast tumor. All the images are collected from 82 different patients out of which 24 for benign and 58 for malignant. Images of each patient are provided in four different magnifications. A detail distribution of images is given in Table 1.

Table 1. Detailed description of BreakHis dataset.

	Magnifications				Total	Patient
	40x	100x	200x	400x		
Benign	625	644	623	588	2480	24
Malignant	1370	1437	1390	1232	5429	58
Total	1995	2081	2013	1820	7909	82

3. Methodology

In this section, we briefly discuss about the following:

1. Colour-texture image descriptors used in the approach.

2. Classifiers used in the approach

3. Majority voting.

3.1. Colour-texture image descriptors

This subsection discusses about the colour-texture features employed for present study. Below, we briefly discuss the utilized colour-texture features:

1. **Normalized colour space representation [16]:** This method calculates the textural (Gabor filter) features from the matrix of complex numbers of the form $(P1+iP2)$, where P1 and P2 are the normalized colour channel values that are chosen based on the range and average values of the colour channels.
2. **Multilayer Coordinate Clusters representation [17]:** This feature describes the textural and colour content of an image by splitting the original colour image into a stack of binary images, where each binary image represents a code based on a predefined palette (quantized colour space).
3. **Gabor features on Gaussian colour model [18]:** The colour-texture feature is calculated in two steps: 1) colour measurement in a transformed colour space based on a Gaussian colour model, and 2) texture measurement through Gabor filter bank.
4. **Gabor chromatic features [19]:** Combination of Gabor features and chromatic features are extracted from the luminance plane.
5. **Complex Wavelet features and chromatic features [20]:** Dual Tree Complex Wavelet Transform (DT-CWT) is computed for each colour channel. It has advantages such as directional selectivity and moderate redundancy over Discrete Wavelet Transform.
6. **Opponent Colour Local Binary pattern (OCLBP) [21]:** It computes LBP for each colour channel (intra channel) separately and for each opponent colour channel $((c_1, c_2), (c_1, c_3)$ and $(c_2, c_3))$ jointly.

For more on colour-texture feature please refer [13].

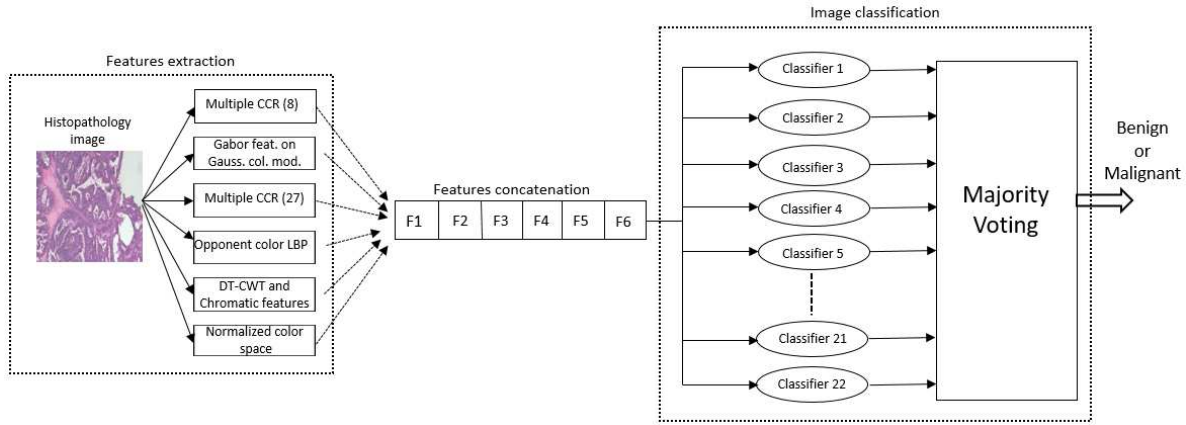


Figure 3. Overall process of image classification.

3.2. Classifiers

We explore various supervised classifiers, for which we provide a short description below [22].

1. **Support Vector Machine (SVM) [23]**: It learns a hyperplane that separates a set of positive examples from a set of negative examples with maximum margin. The hyperplanes can be learnt in higher dimensional space using kernels. Based on the kernel and their parameters, a variety of SVMs can be defined.
 - (a) Linear SVM
 - (b) Quadratic SVM (Quadratic kernel)
 - (c) Cubic SVM (Cubic kernel)
 - (d) Fine Gaussian SVM (Radial Basis Function (RBF) kernel, kernel scale set to $\sqrt{P}/4$)
 - (e) Medium Gaussian SVM (Radial Basis Function (RBF) kernel, kernel scale set to \sqrt{P})
 - (f) Coarse Gaussian SVM (Radial Basis Function (RBF) kernel, kernel scale set to $4\sqrt{P}$)

where P is the number of predictors.

2. **Decision Tree [24]**: It is a graphical representation of possible solutions to a decision based on certain conditions. It usually works in top-down manner, by choosing a variable (feature) at each step that best splits the set into subsets. Various metrics for measuring "best" i.e. measure the homogeneity of the target variable within the subsets are utilized by different algorithms. Some of the metrics are Gini impurity (GI), Information gain (IG) etc. Based on maximum number of splits used in tree, various trees can be defined.
 - (a) Simple Tree (maximum number of splits is 4)
 - (b) Medium Tree (maximum number of splits is 20)

- (c) Complex Tree (maximum number of splits is 100)

3. **Nearest Neighbors classifier [25]** : In this case, test sample is classified by comparing it to the known samples (training) according to some distance/similarity function. Based on number of neighbors and distance metric used, a variety of k-NN exists.

- (a) Fine KNN (number of neighbors is set to 1, euclidean metric)
- (b) Medium KNN (number of neighbors is set to 10, euclidean metric)
- (c) Coarse KNN (number of neighbors is set to 100, euclidean metric)
- (d) Cosine KNN (number of neighbors is set to 10, Cosine distance metric)
- (e) Cubic KNN (number of neighbors is set to 10, cubic distance metric)
- (f) Weighted KNN (number of neighbors is set to 10, distance based weight)

4. **Discriminant Analysis [26]**: Here, one learns multivariate distributions (groups) from the training data. It estimates the distance of each observation to each group's multivariate mean (centroid) using Mahalanobis distance. A new sample is labelled in that group for which the distance is minimum. Based on the boundaries formed between classes, we consider two types of discriminant analysis,

- (a) Linear Discriminant (linear boundaries)
- (b) Quadratic Discriminant (non-linear boundaries such as ellipse, parabola or hyperbola)

5. **Ensemble Classifier [27]** : It is a process by which multiple learners such as classifiers or experts, are

constructed and their output are combined to classify a new sample. The employment of different base learner generation processes and/or different combination schemes leads to different ensemble methods:

- (a) Boosted Tree: Each base estimator is grown to re-weighted versions of the training data (sequentially) in a way that it reduces the bias of the combined estimator. The final classifier will be the weighted average of classifiers.
- (b) Bagged Tree: This is a bootstrap aggregation ensemble of complex decision trees. These decision trees are trained on samples which are drawn with replacement from original data.
- (c) Subspace Discriminant Learner(SDL): Creates an ensemble of discriminant classifiers using the random subspace algorithm where random subsets of features are drawn from the data for training each classifier.
- (d) Subspace KNN: Creates an ensemble of Nearest Neighbors (NN) using random subspace algorithm.
- (e) RUSBoosted Trees: LogitBoost algorithm (which is derived from adaboost) with Decision Tree learners.

3.3. Majority voting

Figure 3 shows the overall classification framework. In proposed framework, we use an ensemble of heterogeneous classifier. To fuse the output of different classifier majority voting is used. Majority voting is a decision rule where the class of new sample is decided based on votes (labels) provided by each classifier to each class. The class which receives the most votes is used as a final label for a test sample. As indicated earlier, the majority voting strategy can be useful in considering classification across magnification levels, as each classifier may discriminate the features differently for each magnifications. Thus, a voting strategy can help towards generalizing the framework for all magnifications.

4. Result & Discussion

In this section, we first discuss some aspects of our experimentation, and then provide and discuss our results. In our experiments, we have randomly chosen 58 patients (70%) for training and remaining 25 for testing (30%). This also enables fair comparison with a state-of-the-art approach [15]. We train the above mentioned classifiers using images for the chosen 58 patients, and also used five trials of random selection of training-testing data. These trained models are tested using images of the remaining images 25 patients. In subsequent subsections, we will discuss the evaluation metrics used to compute our results.

4.1. Evaluation metric

To compare results with existing approach, we also use patient recognition rate (PRR) as evaluation metric. The definition of patient recognition rate is given as follows:

$$PRR = \frac{\sum_{i=1}^N PS_i}{N} \quad (1)$$

where N is the total number of patients (available for testing). The patient score is define as follows,

$$PS = \frac{N_{rec}}{N_P} \quad (2)$$

where N_{rec} and N_P are the correctly classify and total cancer image of patient P respectively.

4.2. Performance of the magnification independent model, and related comparison

To validate the effectiveness of proposed framework (the use of colour-texture features and the ensemble-classifier framework with voting), we first compare the results obtained from magnification independent model with the state-of-the-art approach [15], which is based on deep learning. To our knowledge, this is only work on BreakHis dataset which considers a magnification independent model. The results are provided in Table 2. We can observe from the table that, proposed method outperforms the existing approach, when testing at all magnification levels. Furthermore, one can also observe that the proposed work yields a lesser variance in scores, in most of the cases. This experiments validates the effectiveness of our framework.

Table 2. Performance Comparison.

Methods/Magnification	Recognition Rate based on patient score (%)				
	40X	100X	200X	400X	Average
Bayramoglu et al. [15]	83.08±2.08	83.17±3.51	84.63±2.72	82.10±4.42	83.25
Proposed Method	87.2±3.74	88.22±3.28	88.89±2.51	85.82±3.81	87.53

Table 3. Inter-magnification classification performance with the magnification-specific models

Training Magnification	Training Magnification				Average testing performance over all magnifications
	40X	100X	200X	400X	
40X	84.89	83.24	81.15	70.47	79.93
100X	87.38	86.19	86.22	88.69	87.12
200X	86.38	86.44	86.48	84.8	86.53
400X	85.05	84.37	86.37	82.92	84.68

4.3. Performance of magnification specific models

Having established the experimental validity of our classification approach, we next illustrate in Table 3 the average results (over 5 random trials) obtained for inter-magnification classification for magnification-specific models. From the Table 3, we can observe that extreme magnification (40X, 400x) has relatively lower accuracy and also

relatively larger variation in accuracy, as compared to the mid-range magnifications (100x, 200x), which have more consistent results. The reason could be the large difference in texture properties of image patterns.

For example, 40X specific model gives inferior performance when tested with images of 400X due to the large variation in patterns on which model was trained and tested. It can also be expected that the mid-range magnifications (100X, 200X) may have lesser variability among features with other magnifications. Interestingly, the average accuracy for the (100X, 200X) specific models across all magnifications (Table 3), is similar to the average accuracy of the magnification independent case (Table 2).

However, there are also some unexpected results. For instance, the performance drop observed in the 40X specific model for the 400X testing images, is not reciprocated in the 400X specific model. Also, in some cases, the testing with images with the same magnification as the training model, does not yield the highest results.

4.4. Performance across classifiers

To further gain some more insight about the inter-magnification classification, we provide in Table 4 and Table 5, some quantitative results across the various classifiers used in this work. One can note that, the mean accuracy over the various classifiers for magnification-specific models is not too high. However, the majority voting results are much higher. Hence, clearly the framework of using an ensemble-classification with a voting scheme seems to be playing a role in achieving the good performance across magnifications.

In this case to we note that for 100X and 200X magnifications, the mean across classifiers is consistently high, and the standard deviation low. This observation further supports the earlier one that the 100x and 200x models, seem to yield better magnification invariant performance (with 100X being somewhat better and consistent than 200X). We also report the number of high performing classifiers for each model. We define these are the classifiers which have the accuracy $\geq 80\%$. Even in this case, we notice that the 100X and 200X models have a large number of high performing classifiers (again with 100x better than 200X).

When comparing such quantities for magnification specific models (Table 4) with those of magnification independent model Table 5, we note that the latter has a higher mean, lesser standard deviation, and a large number of high-performing classifiers. Thus, as expected, in terms of individual classifiers, the magnification independent model is certainly more consistent than training with just one magnification. However, with an ensemble classification, the overall performance of the magnification specific models comes close to that of the magnification independent one, especially for 100X and 200X cases.

Finally, we note that the highest classification performance in Table 4 and Table 5 is often higher than the majority voting performance. However, there are some differences in the classifiers which yield this highest classification performance. Thus, no single classifier is the best for all cases (although, we have observed that there are a few who are better than many). This further suggests the case in support of an ensemble classifier framework.

4.5. Conclusion

In this work, we proposed the use of colour-texture features and an ensemble classifier framework for classification of breast cancer histopathology images. While we demonstrated the effectiveness of using such features and classification, importantly, we provided various experimental studies which indicates some interesting aspects about the role of optical magnification in classification. From our experiments, it is apparent that with suitable features within an ensemble classification framework, the classification can be made largely magnification invariant, more so for magnification factors than others. The magnification models learnt in this manner yield performance similar to the magnification independent model. We believe that this is an interesting study which raises some questions about scale-invariance properties of feature-classifier combination, role of ensemble classification, considering that the magnification specific model requires relatively less training than the magnification independent model, considering certain observed asymmetries in the results etc. It can also have important practical implications for breast cancer histopathology diagnosis systems.

References

- [1] American Cancer Society. Breast cancer facts & figures 2011-2012. *American Cancer Society INC.*, 1(34), 2011.
- [2] C Loukas, Spiros Kostopoulos, Anna Tanoglidi, Dimitris Glotsos, C Sfikas, and Dionisis Cavouras. Breast cancer characterization based on image classification of tissue sections visualized under low magnification. *Computational and mathematical methods in medicine*, 2013.
- [3] Mitko Veta, Josien PW Pluim, Paul J Van Diest, and Max A Viergever. Breast cancer histopathology image analysis: A review. *IEEE Transactions on Biomedical Engineering*, 61(5):1400–1411, 2014.
- [4] Metin N Gurcan, Laura E Boucheron, Ali Can, Anant Madabhushi, Nasir M Rajpoot, and Bulent Yener. Histopathological image analysis: A review. *IEEE reviews in biomedical engineering*, 2:147–171, 2009.
- [5] Yungang Zhang, Bailing Zhang, Frans Coenen, and Wenjin Lu. Breast cancer diagnosis from biopsy images with highly reliable random subspace classifier ensembles. *Machine vision and applications*, 24(7):1405–1420, 2013.

Table 4. Classifier performance analysis for magnification specific model.

Performance metric	Magnification specific model (40X)				Magnification specific model (100X)			
	Testing magnification				Testing magnification			
	40X	100X	200x	400X	40X	100x	200x	400x
Mean accuracy across all classifier	80.40	78.69	77.15	71.03	82.01	82.21	82.80	80.07
Standard deviation across all classifier	2.99	5.06	6.50	8.00	3.04	3.57	3.04	3.81
Maximum accuracy	84.96 (Coarse KNN)	87.44 (Boosted Tree)	88.02 (Boosted Tree)	85.86 (Boosted Tree)	87.85 (Bagged Tree)	88.47 (Simple Tree)	89.35 (Bagged Tree)	86.71 (Bagged Tree)
Majority Voting	84.89	83.24	81.15	70.47	87.38	86.19	86.22	88.69
High performance classifiers	12	6	6	4	18	18	19	12
Performance metric	Magnification specific model (200X)				Magnification specific model (400X)			
	Testing magnification				Testing magnification			
	40X	100X	200X	400X	40X	100X	200X	400X
Mean accuracy across all classifier	78.02	79.83	83.14	80.65	75.98	77.49	81.23	80.01
Standard deviation across all classifier	5.98	4.86	2.49	3.20	5.95	6.77	5.09	4.53
Maximum accuracy	86.80 (Bagged Tree)	87.47 (Bagged Tree)	88.32 (Bagged Tree)	86.11 (Bagged Tree)	86.26 (Boosted Tree)	89.17 (Boosted Tree))	88.48 (Boosted Tree)	86.40 (Boosted Tree)
Majority Voting	86.38	86.44	86.48	84.8	85.05	84.37	86.37	82.92
High performance classifiers	9	10	20	13	6	8	15	9

Table 5. Classifier performance analysis for magnification independent model.

Performance metric	Magnification-independent model			
	Testing magnification			
	40X	100X	200x	400X
Mean accuracy across all classifier	82.98	83.68	84.84	83.22
Standard deviation across all classifier	2.6	2.99	2.09	2.59
Maximum accuracy	86.96 (Bagged Tree)	88.92 (Bagged Tree)	90.32 (Bagged Tree)	86.85 (Bagged Tree)
Majority Voting	87.2	88.22	88.89	85.82
High performance classifiers	19	19	21	18

[6] Yungang Zhang, Bailing Zhang, Frans Coenen, Jimin Xiao, and Wenjin Lu. One-class kernel subspace ensemble for

medical image classification. *EURASIP Journal on Advances in Signal Processing*, 2014(1):17, 2014.

[7] Claus Bahlmann, Amar Patel, Jeffrey Johnson, Jie Ni, Andrei Chekkoury, Parmeshwar Khurd, Ali Kamen, Leo Grady, Elizabeth Krupinski, Anna Graham, et al. Automated detection of diagnostically relevant regions in h&e stained digital pathology slides. In *SPIE Medical Imaging*, pages 831504–831504. International Society for Optics and Photonics, 2012.

[8] Eric Cosatto, Matt Miller, Hans Peter Graf, and John S Meyer. Grading nuclear pleomorphism on histological micrographs. In *Pattern Recognition, 2008. ICPR 2008. 19th International Conference on*, pages 1–4. IEEE, 2008.

[9] Nina Linder, Juho Konsti, Riku Turkki, Esa Rahtu, Mikael Lundin, Stig Nordling, Caj Haglund, Timo Ahonen, Matti

- Pietikäinen, and Johan Lundin. Identification of tumor epithelium and stroma in tissue microarrays using texture analysis. *Diagnostic pathology*, 7(1):22, 2012.
- [10] Fabio A Spanhol, Luiz S Oliveira, Caroline Petitjean, and Laurent Heutte. A dataset for breast cancer histopathological image classification. *IEEE Transactions on Biomedical Engineering*, 63(7):1455–1462, 2016.
- [11] Fabio Alexandre Spanhol, Luiz S Oliveira, Caroline Petitjean, and Laurent Heutte. Breast cancer histopathological image classification using convolutional neural networks. In *Neural Networks (IJCNN), 2016 International Joint Conference on*, pages 2560–2567. IEEE, 2016.
- [12] Alex Krizhevsky, Ilya Sutskever, and Geoffrey E Hinton. Imagenet classification with deep convolutional neural networks. In *Advances in neural information processing systems*, pages 1097–1105, 2012.
- [13] Francesco Bianconi, Richard Harvey, Paul Southam, and Antonio Fernández. Theoretical and experimental comparison of different approaches for color texture classification. *Journal of Electronic Imaging*, 20(4):043006–043006, 2011.
- [14] Dana E Ilea and Paul F Whelan. Image segmentation based on the integration of colour–texture descriptors a review. *Pattern Recognition*, 44(10):2479–2501, 2011.
- [15] Neslihan Bayramoglu, Juho Kannala, and Janne Heikkilä. Deep learning for magnification independent breast cancer histopathology image classification.
- [16] Constantin Vertan and Nozha Boujemaa. Color texture classification by normalized color space representation. In *Pattern Recognition, 2000. Proceedings. 15th International Conference On*, volume 3, pages 580–583. IEEE, 2000.
- [17] Francesco Bianconi, Antonio Fernández, Elena González, Diego Caride, and Ana Calviño. Rotation-invariant colour texture classification through multilayer ccr. *Pattern Recognition Letters*, 30(8):765–773, 2009.
- [18] Minh A Hoang, Jan-Mark Geusebroek, and Arnold WM Smeulders. Color texture measurement and segmentation. *Signal processing*, 85(2):265–275, 2005.
- [19] Alexandru Drimbarean and Paul F Whelan. Experiments in colour texture analysis. *Pattern recognition letters*, 22(10):1161–1167, 2001.
- [20] Maria E Barilla and Michael Spann. Colour-based texture image classification using the complex wavelet transform. In *Electrical Engineering, Computing Science and Automatic Control, 2008. CCE 2008. 5th International Conference on*, pages 358–363. IEEE, 2008.
- [21] Topi Mäenpää and Matti Pietikäinen. Texture analysis with local binary patterns. *Handbook of Pattern Recognition and Computer Vision*, 3:197–216, 2005.
- [22] Classification-learner-app. <https://in.mathworks.com/help/stats/classification-learner-app.html>.
- [23] Chih-Chung Chang and Chih-Jen Lin. Libsvm: a library for support vector machines. *ACM Transactions on Intelligent Systems and Technology (TIST)*, 2(3):27, 2011.
- [24] Lior Rokach and Oded Maimon. Top-down induction of decision trees classifiers-a survey. *IEEE Transactions on Systems, Man, and Cybernetics, Part C (Applications and Reviews)*, 35(4):476–487, 2005.
- [25] Naomi S Altman. An introduction to kernel and nearest-neighbor nonparametric regression. *The American Statistician*, 46(3):175–185, 1992.
- [26] Geoffrey McLachlan. *Discriminant analysis and statistical pattern recognition*, volume 544. John Wiley & Sons, 2004.
- [27] Lior Rokach. Ensemble-based classifiers. *Artificial Intelligence Review*, 33(1-2):1–39, 2010.